Abbreviations

%N	percentage nitrogen by mass
2-NDPA	2-Nitrodiphenylamine
AIMD	*ab initio* molecular dynamics
AO	atomic orbital
a.u.	atomic units
B3LYP	Becke, 3-parameter, Lee-Yang-Parr hybrid functional
BCP	bonding critical point
BSSE	basis set superposition error
CH_3/CH_3	NC repeat unit with two $-OCH_3$ capping groups
CH_3/OH	NC repeat unit with $-OCH_3$ capping group on ring 1 and $-OH$ group on ring 2
OH/CH_3	NC repeat unit with $-OH$ capping group on ring 1 and $-OCH_3$ group on ring 2
CCP	cage critical point
CP	critical point
DFT	density functional theory
DFT-D	density functional theory with dispersion correction
DSC	differential scanning calorimetry
DOS	degree of substitution

DPA diphenylamine

EN ethyl nitrate

ESP electrostatic potential

FF force field

G09 Gaussian 09 revision E.01

GGA generalised gradient approximation

GM genetically modified

GTO Gaussian type orbitals

GView Gauss View 5.0.8

HF Hartree-Fock

HMF hydroxymethylfurfural

HOMO highest occupied molecular orbital

IR infra-red spectroscopy

KS-DFT Kohn-Sham DFT

LDA local density approximation

MD molecular dynamics

MEP minimum energy path

MM molecular mechanics

MMFF94 Merck molecular force field 94

MO molecular orbitals

MP2 Møller–Plesset perturbation theory with second order correction

MW molecular weight

NBO natural bond orbital

NC	nitrocellulose
NCP	nuclear critical point
NG	nitroglycerine
NMR	nuclear magnetic resonance spectroscopy
PCM	polarisable continuum model
PES	potential energy surface
PETN	pentaerythritol tetranitrate
PETRIN	pentaerythritol trinitrate
QM	quantum mechanics
QTAIM	quantum theory of atoms in molecules
RCP	ring critical point
RESP	restrained electrostatic potential atomic partial charges
RHF	restricted HF
RMS	root mean square
ROHF	restricted-open HF
UHF	unrestricted HF
SB59	1,4-bis(ethylamino)-9,10-anthraquinone dye
SCF	self-consistent field
SCRF	self-consistent reaction field
SEM	scanning electron microscopy
SMD	solvation model based on density
S_N2	bi-molecular nucleophilic substitution reaction
STO	Slater type orbitals

TG	thermogravitmetric analysis
TS	transition state
UFF	universal force field
UV	ultraviolet
UV-vis	ultraviolet–visible spectroscopy
vdW	van der Waals
ωB97X-D	ωB97X-D long-range corrected hybrid functional
ZPE	zero-point energy

Chapter 1

Conclusion and future work

1.1 Conclusion

Since winning a medal at the World's Fair in London in 1862 as the first man-made plastic [1, 2], nitrocellulose (NC) has become a central component in the manufacturing of everyday items across a whole spectrum of critical applications, from kitchenware to rocket fuel [3]. As has been demonstrated by this study and the extensive years of research since its first discovery, the degradation behaviour of NC is multi-staged and subject to high variation. The interplay of thermal triggers, hydrolytic initiation, as well as other factors not discussed here such as ultraviolet (UV) initiation [4, 5] and physical shock [6], are all subject to the unique composition of each sample; variation owed to its biological origins and preparation method. Adding to this, the ageing reactions that occur are at the mercy of the precise environmental conditions under which the NC is stored. The final result is that the true, exhaustive reaction scheme for full decomposition has remained elusive.

In this thesis, the degradation processes in NC were explored using computational methods to elucidate the dominant processes and key reactants involved in ambient ageing. In the first section, the polymeric structure of NC was introduced. Different sized truncations and capping group approximations for polymer chain endings were tested as models for the polysaccharide. This was achieved by inspection of the partial charges, electrostatic potential (ESP) and critical interaction points for monomeric, dimeric and trimeric β-glucopyranose structures. The dimer was found to be the minimum structure required to reproduce the full properties of NC within a repeat unit.

Methoxy and hydroxyl capping groups were compared; the methoxy groups provided a more sterically and chemically similar proxy for the extended polymer, following examination of charges and geometry dependent interactions. Comparison of the charge densities

and intramolecular interactions around the monomer and dimer revealed that the former exhibited an acceptable level of deviation from the dimer behaviour, particularly with reference to further investigations concentrating only on localised reaction interactions. The bi-methoxy monomer was implemented as the model for NC in later studies.

Using the monomer model, the primary steps of decomposition were explored in Chapter **??**. Thermolytic denitration reactions were investigated; homolytic fission of the nitrate $O-NO_2$ bond, and elimination of HNO_2 were tested for both the PETN test case, and the NC monomer model. Good agreement with literature values was found for the reaction energies and activation energies, in case of HNO_2 elimination in both pentaerythritol tetranitrate (PETN) and NC. The loss of $\bullet NO_2$ *via* homolysis was confirmed. For the acid hydrolysis pathway , possible protonation sites in the monomer were analysed. It was found that the proton site most amenable to denitration was the bridging oxygen position of the nitrate. Further investigations considered denitration routes beginning from isomers protonated at both the terminal (upper) and bridging sites. The denitration step was then explored *via* a series of potential energy surface (PES) scans. The stability of different possible transition state (TS) ring structures involving both pre-protonation and concerted protonation-denitration was examined, in addition to the nature of the NO_2 leaving group. No stable TS structures presenting the correct vibration for denitration were isolated, however scans confirmed that the NO_2 was released as NO_2^+, with possible formation of HNO_2 at greater separations.

Proposed decomposition routes originating from the primary denitration step were collated from nitrate ester reactions in literature. Using ethyl nitrate (EN) as an initial test case, the energies of each reaction were evaluated to determine whether it were a viable secondary reaction step following liberation of the $\bullet NO_2$, NO_2^+ or HNO_2 following first stage decomposition. Possible decomposition schemes were constructed, mapping from the point of NO_2 liberation to the oxidation of the alcohol group. The reaction energies were determined for the NC monomer. It was found that the energies were largely favourable from a thermodynamic equilibrium perspective. The fate of the released nitrogen species was in the accumulation of N_2O or regeneration of $\bullet NO_2$, suggesting $\bullet NO_2$ as the species responsible for autocatalytic processes in the system. Consumption of $\bullet NO_2$ in the formation of acids proved to be thermodynamically unfavourable.HNO_2 routes lead to the formation of N_2O without self-regeneration and HNO_3 routes lead primarily to formation of $\bullet NO_2$. This

indicates that HNO_2 was unlikely to be a direct contributor to catalysis, and that HNO_3 was the precursor to the $\bullet NO_2$ catalytic species, acknowledging experimental observations that HNO_3 appeared to facilitate autocatalysis [7].

Following the successful application of the monomer model in the investigation of denitration and protonation reactions of NC, further studies repeating the mechanisms explored here using the dimer (and trimer models, where feasible) would be extremely valuable. Possible synergistic effects of neighbouring nitrate groups on adjacent rings, in addition to increased steric factors, are likely to change the energetics and favourability of attack and protonation sites, thus altering the likelihood of denitration at each ring position. Inter-chain hydrogen bonding, largely dependent on unsubstituted hydroxyl groups, is also likely to alter the contribution to hydrolysis in particular. Porosity to solvents is influenced by local crystallinity and packing [8, 9], and is sensitive to the spatial arrangements of individual hydroxyl groups [10, 11, 12]. Molecular packing will determine the ease at which liberated degradation products can diffuse through and escape the NC matrix. It can be surmised that there exists certain decomposition pathways with corresponding reactions that are solely structure dependent.

Whilst this work has not exhaustively explored the myriad reactions that may occur in the complex ageing procedures of NC, it has established the key reactions of the early stages of degradation, with presentation of an effective truncation of the polymeric structure applicable for further study in the topic. Key competing reactions for the denitration step, the identity of nitrogen species released and their role in the longer-range decomposition process has been presented. The conclusion of this project sets the scope for subsequent investigations into the later-stage reaction processes that lead to deeper degradation of the NC backbone.

1.2 Further Work

In addition to expansion of the NC model to larger dimer and trimer units, the existing NC model may be refined by conducting a more rigorous examination of the subtle variations in geometry. Conformational scans, in particular for the C6 chain and for the orientation of the rings within the trimer, would benefit identification of other low energy structures likely to be present in the natural polymer. Here, only the denitration schemes for the singly nitrated NC monomer were documented. The differing stabilities of NC at varying levels of nitration will undoubtedly affect the reactivity at each site. Propagation of different nitration

level and conformational structures through the denitration and secondary decomposition schemes may reveal alternative reactions, or alter the balance of products obtained.

Classical molecular dynamics (MD) techniques would also provide further insight into the diffusion of the released products, and their interaction with the wider polymer. Studies involving the interaction of NC with plasticisers has effectively probed the diffusion rates of plasticiser migration, which is of key interest in the preservation of stable NC product formulations [13].

Another avenue of interest is in the exploration of other transition structures for the denitration stage, and for further degradation following formation of the ketone. The inclusion of additional explicit water molecules or water clusters is likely required to stabilise TS that were previously not viable (chapter **??** figure **??**), highlighting the need for further understanding of NC-solvent interactions. A starting reference work would be the modelling of pentahydrate complexes around glucose by Momany *et al.* [**?**], with extension to a hybrid quantum mechanics/molecular mechanics (QM/MM) approach to treatment of solvation shells. Ab-initio molecular dynamics (AIMD) techniques may be effective for investigation into the interactions of both water and acids with NC, offering possible insight into the effect of increasing acid concentration on the protonation behaviour and water clustering around monomer, dimer and trimer structures at different degree of substitution (DOS) [14].

A natural extension to the study of the secondary reactions driving decomposition is the expansion to a wider range of possible reaction pathways. These may include the widely documented mechanisms studied for glucose, such as the conversion to hydroxymethyfurfural (HMF), whereby the 6-membered ring is converted to a 5-membered ring (figure 1.1) [15, 16, 17]; furan and other aromatic species have been observed in NC degradation residues [18]. This is in addition to further studies of possible ring opening mechanisms and chain scission reactions, in order to fully account for the broad spectrum of experimentally observed degradation products in infra-red spectroscopy (IR) and nuclear magnetic resonance spectroscopy (NMR) measurements [19, 20, 21, 22, **?**].

Figure 1.1: The conversion of glucose to hydroxymethylfurfural (HMF) with a) showing the proposed reaction scheme, and b) displaying a possible mechanistic pathway, from the *ab initio* molecular dynamics (AIMD) study by Qian *et al.* [23].

(a) Conversion of glucose (I) to HMF (III) *via* a furan aldehyde intermediate (II).

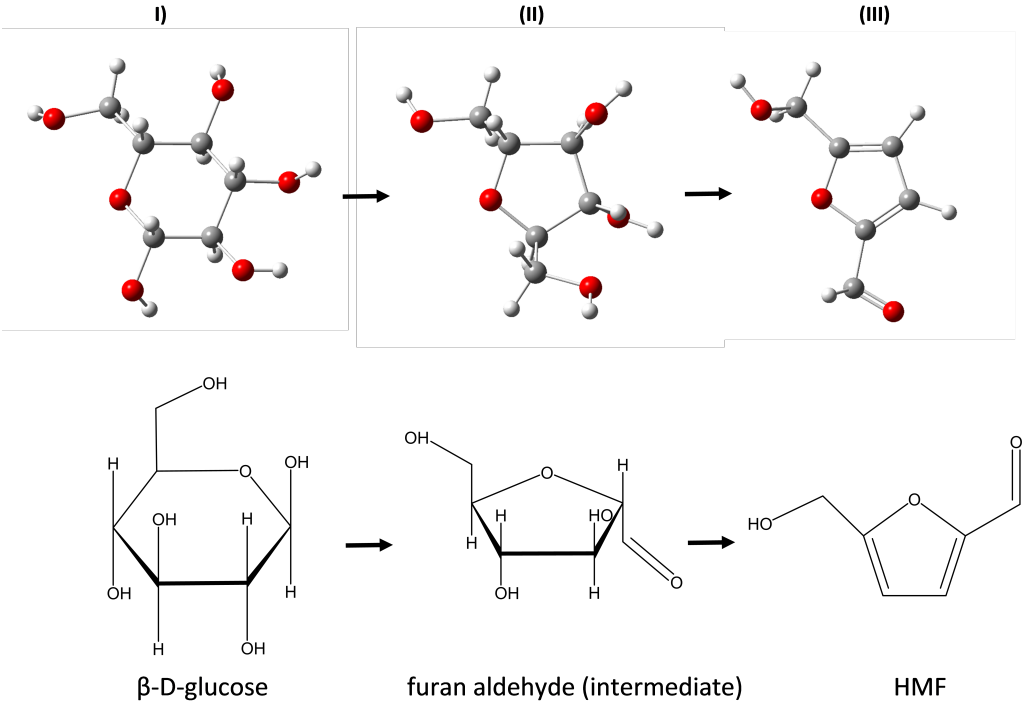

(b) (1): Protonation of C2−OH on β-D-glucose, (2): breakage of the C2−O2 Bond, (3): the formation of the C2−O5 bond during glucose conversion to HMF.

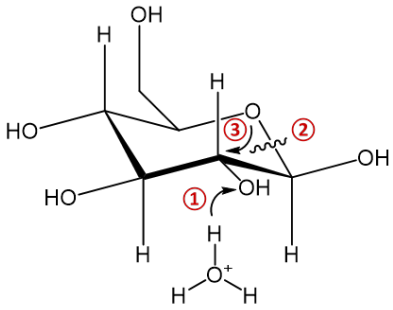

Bibliography

[1] Deac Rossell. Exploding teeth, unbreakable sheets, and continuous casting : Nitrocellulose, from guncotton to early cinema. *This Film is Dangerous*, 2002.

[2] Alexander Parkes. Parkesine replica of bronze medal awarded to alexander parkes at the international exhibition in 1862. 1862. Replica medal. Object number: 2009-177.

[3] A. S. Greenberg and Simon Broder. The story of nitrocellulose. *Journal of the Patent Office Society*, 8(11):517–529, 1925.

[4] Sebastien Berthumeyrie, Steeve Collin, Pierre-Olivier Bussiere, and Sandrine Therias. Photooxidation of cellulose nitrate: New insights into degradation mechanisms. *Journal of Hazardous Materials*, 272:137–147, 2014.

[5] V. A. Khryachkov, E. A. Saratovskikh, R. N. Yarullin, and A. V. Kulikov. Effect of the d. desulfuricans bacterium and uv radiation on nitrocellulose oxidation. *Russian Journal of Physical Chemistry B*, 11(4):697–703, 2017.

[6] A. J. Taylor. Explosibility hazard of unpigmented industrial nitrocellulose. Technical Report 1, Royal Armament Research and Development Establishment, Ministry of Defence, UK, September 1971.

[7] John W. Baker and D. M. Easty. 217. hydrolytic decomposition of esters of nitric acid. part i. general experimental techniques. alkaline hydrolysis and neutral solvolysis of methyl, ethyl, isopropyl, and tert.-butyl nitrates in aqueous alcohol. *J. Chem. Soc.*, (0):1193–1207, 1952.

[8] David M. French. The density of cellulose nitrate. *J. Appl. Polym. Sci.*, 22(1):309–313, January 1978.

[9] D. T. Clark and P. J. Stephenson. A 13c n.m.r. and x-ray study of the relationship between the distribution of nitrate ester groups and interchain d(110) spacings in a series of cellulose nitrates. *Polymer*, 23(9):1295–1299, 1982.

[10] R. G. Zhbankov. Hydrogen bonds and structure of carbohydrates. *Journal of Molecular Structure*, 270:523–539, 1992.

[11] Margaretha Akerholm, Barbara Hinterstoisser, and Lennart Salmen. Characterization of the crystalline structure of cellulose using static and dynamic ft-ir spectroscopy. *Carbohydrate Research*, 339(3):569–578, 2004.

[12] Yoshiharu Nishiyama, Paul Langan, and Henri Chanzy. Crystal structure and hydrogen-bonding system in cellulose iβ from synchrotron x-ray and neutron fiber diffraction. *J. Am. Chem. Soc.*, 124(31):9074–9082, August 2002.

[13] Lisa A. Richards, Anthony Nash, Maximillian Joshua Sebastian Phipps, and Nora H. de Leeuw. A molecular dynamics study of plasticiser migration in nitrocellulose binders. *New J. Chem.*, 42(21):17420–17428, 2018.

[14] Diego Ardura and D. J. Donaldson. Where does acid hydrolysis take place? *Phys. Chem. Chem. Phys.*, 11(5):857–863, 2009.

[15] Xianghong Qian, Mark R. Nimlos, David K. Johnson, and Michael E. Himmel. Acidic sugar degradation pathways. In Brian H. Davison, Barbara R. Evans, Mark Finkelstein, and James D. McMillan, editors, *Twenty-Sixth Symposium on Biotechnology for Fuels and Chemicals*, pages 989–997. Humana Press, Totowa, NJ, 2005.

[16] Xianghong Qian, Mark R. Nimlos, Mark Davis, David K. Johnson, and Michael E. Himmel. Ab initio molecular dynamics simulations of β-d-glucose and β-d-xylose degradation mechanisms in acidic aqueous solution. *Carbohydrate Research*, 340(14):2319–2327, 2005.

[17] Xianghong Qian, David K. Johnson, Michael E. Himmel, and Mark R. Nimlos. The role of hydrogen-bonding interactions in acidic sugar reaction pathways. *Carbohydrate Research*, 345(13):1945–1951, 2010.

[18] Tomas L. Jensen, John F. Moxnes, Erik Unneberg, and Ove Dullum. Calculation of decomposition products from components of gunpowder by using reaxff reactive

force field molecular dynamics and thermodynamic calculations of equilibrium composition. *Propellants, Explosives, Pyrotechnics*, 39(6):830–837, December 2014.

[19] Liu Huwei and Fu Ruonong. Studies on thermal decomposition of nitrocellulose by pyrolysis-gas chromatography. *Journal of Analytical and Applied Pyrolysis*, 14(2):163–169, 1988.

[20] D. T. Clark, P. J. Stephenson, and F. Heatley. Partial degrees of substitution in cellulose nitrates determined by means of 13c magnetic resonance studies. *Polymer*, 22(8):1112–1117, 1981.

[21] L. Dauerman and Y. A. Tajima. Thermal decomposition and combustion of nitrocellulose. *AIAA Journal*, 6(8):1468–1473, August 1968.

[22] V. I. Kovalenko, R. M. Mukhamadeeva, L. N. Maklakova, and N. G. Gustova. Interpretation of the ir spectrum and structure of cellulose nitrate. *Journal of Structural Chemistry*, 34(4):540–547, 1994.

[23] Xianghong Qian. Mechanisms and energetics for acid catalyzed β-d-glucose conversion to 5-hydroxymethylfurfurl. *J. Phys. Chem. A*, 115(42):11740–11748, October 2011.